Optical vibrations of hydrogen in some rare-earth monohalide hydrides



1994 J. Phys.: Condens. Matter 6 4053

(http://iopscience.iop.org/0953-8984/6/22/005)

J. Phys.: Condens. Matter 6 (1994) 4053–4066. Printed in the UK

# Optical vibrations of hydrogen in some rare-earth monohalide hydrides

R K Kremer†, J K Cockcroft†§, Hj Mattausch†, A Simon† and G J Kearley‡

† MPI für Festkörperforschung, Heisenbergstrasse 1, W-70506 Stuttgart 80, Germany

‡ Institut Laue-Langevin, 156X, 38042 Grenoble Cédex, France

Received 27 January 1994

**Abstract.** We report an investigation of the local modes of hydrogen and deuterium atoms by means of inelastic neutron scattering at 10 K and 100 K in some hydride and deuteride monohalides of the rare-earth elements, REXH$_x$, with RE = Y and Tb, X = Cl and Br and $x \simeq 0.8$. These compounds contain hydrogen/deuterium atoms in distorted tetrahedral metal-atom voids. The hydride spectra exhibit two modes centred at about 125 meV and 90 meV for YBrD$_x$. For the deuterium compounds YBrD$_x$ ($x \simeq 0.8$) second-harmonic transitions are observed. The energy splitting of the two modes is of the order of 6–10 meV. The low-energy mode is about twice as intense as the high-energy mode. The splitting of the modes is consistent with local $C_{3v}$ symmetry and analysed in terms of a model suggested recently by Bennington *et al* . Broadenings of the modes are observed and attributed to a weak splitting of the doubly degenerate low-energy mode due to a reduction of local symmetry. To relate the spectra to crystallographic properties a powder neutron-diffraction experiment and a refinement of the crystal structure of YBrD$_{0.79}$ have also been performed.

## 1. Introduction

The investigation of localized-mode vibrational frequencies of hydrogen in metal hydrides by inelastic neutron spectroscopy provides essential information about the effective hydrogen single-particle potential [1]. The magnitude of the vibrational energies allows extraction of the force constants of the single-particle potential. The number of vibrational modes and their degeneracies are determined by the local symmetry of the lattice site occupied by the H atom and thus give valuable structural information.

Hydrogen vibrational neutron spectroscopy has been extensively employed on hydrides of transition metals and transition metal intermetallic compounds [2]. A great deal of experimental information is available for these systems. Comparatively less is known about rare-earth hydride systems [3]. A number of investigations have been carried out on the light rare-earth hydrides (and deuterides) REH(D)$_x$ (RE = La, Ce, Pr, Nd) with $x \simeq 2$ as well as on the non-stoichiometric hydrides with $2 < x < 3$. The rare – earth dihydrides, with the exceptions of $EuH_2$ and $YbH_2$, crystallize in the $CaF_2$ – type structure with the hydrogen atoms occupying the tetrahedrally coordinated lattice sites. Particular interest was paid to the question of additional occupation of octahedrally coordinated lattice sites for $x \rightarrow 2$. Due to the limited sensitivity of neutron diffraction experiments vibrational spectroscopy has some advantage in identifying hydrogen on octahedral sites and has contributed significantly in clarifying the situation [4].

§ Present address: Birkbeck College, University of London, Malet Street, London WC1E 7HX, UK

0953-8984/94/224053+14$19.50  

Generally, the neutron vibrational spectra of the rare-earth dihydrides consist of a strong optical mode between 100 and 130 meV which is attributed to the vibrations of hydrogen atoms on tetrahedral lattice sites. Hydrogen atoms occupying the octahedral sites give rise to a mode at considerably lower energies due to the larger metal-to-hydrogen distances. Typically, energies around 60 meV are found for these modes.

It was first noticed by Sakamoto that the energies of the local modes for sites of a given geometry correlate with the metal–hydrogen distance [5]. On the other hand, when comparing systems with different site geometries considerable differences even for the same metal–hydrogen distances can be observed.

A correlation of the mean frequency of the optical peak for various rare-earth dihydrides with the unit cell dimensions was carried out by Hunt and Ross and Ross *et al* [6,7]. A $1/R$ behaviour of the energy with $R$ being the metal–hydrogen distance was inferred for the La, Ce, Pr and Ho dihydrides. A subsequent analysis of systems with the fluorite-type structure based on a more extensive set of examples including transition-metal dihydrides, in contrast, gave evidence for a power-law dependence, $E(R) = kR^{-x}$ with $x \simeq 1.5$, of the vibrational energies $E$ on the metal–hydrogen distance $R$.

Recently, the investigation of the optical modes of hydrogen dissolved in HCP rare-earth metals has attracted particular interest. Some rare-earth metals such as e.g. Sc, Y, Lu are able to retain substantial amounts of hydrogen in solid solution down to very low temperatures without precipitating an ordered hydride phase. Short-range ordering of hydrogen pairs and the formation of a hydrogen glass seems to be the microscopical mechanism for these unusual behaviours [8].

Here, we shall present the results of our neutron spectroscopy investigations of the optical modes of hydrogen and deuterium in some monohalides of the rare-earth elements. Hydride monohalides of the rare-earth elements with chemical formula $REXH_x$ (RE = rare-earth metals; X = Cl, Br, I; $0.67 < x < 1.0$) have been synthesized recently and their physical properties are currently intensively investigated [9].

These compounds have a layered-type crystal structure and represent highly anisotropic metals with orders of magnitude higher conductivity within the layers than perpendicular to it. Particularly, the Tb and Gd hydride monohalides exhibit a number of very interesting magnetic and electrical properties which are intimately related to the presence of hydrogen in these compounds [10, 11]. In addition, since hydrogen transfer processes between neighbouring metal-atom bilayers are suppressed the monohalides of the rare-earth elements represent interesting examples to study two-dimensional hydrogen diffusion. Recently, it was shown by quasielastic neutron spectroscopy that a diffusion model which assumes that the hydrogen atoms pass through octahedral sites during the diffusive jumps is more appropriate than a model relying on direct jumps between nearest-neighbour tetrahedral sites only [12]. In the crystal structure of the $REXH_x$-type compounds (RE = rare-earth metals; X=Cl, Br, I; $0.67 < x < 1.0$) close-packed metal-atom bilayers that are sandwiched between X-atom layers can be identified as the basic structural units (figure 1). Such X–RE–RE–X sheets stack and are held together via van der Waals forces. According to neutron diffraction studies the H atoms are located within the metal-atom bilayer and within experimental resolution are found to occupy the tetrahedral voids as they do in the rare-earth dihydrides [13]. Filling all tetrahedral voids corresponds to $x = 1.0$. Vacancies in the H substructure give rise to $x < 1$. At the lower end of the compositional range, $x \simeq 0.67$, about one third of the possible H-atom sites are vacant. No indication of vacancy ordering was obtained in the neutron-diffraction experiments [14]. Different stacking sequences of the X–RE–RE–X sheets can occur and leads to different structural types. However, this does not alter the nearest-neighbour metal-atom coordination of the hydrogen atoms.

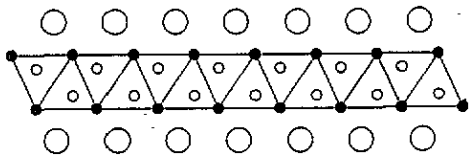

**Figure 1.** Projection along [100] of an X–RE–(H,D)–RE–X sheet cut out of the crystal structure of the rare-earth monohalide hydrides REX(H,D)$_x$ (RE = rare-earth metal atom; X = Cl,Br; $x = 1$). Small circles: (H,D); medium circles: RE; large circles: X. The $c$-axis is perpendicular to the sheet.

In the hydride monohalides of the rare-earth elements the metal-tetrahedron environment of the hydrogen atoms is slightly compressed along a threefold axis (the crystallographic $c$-axis). The degeneracy of the optical modes expected for hydrogen surrounded by a perfect tetrahedral cage is therefore lifted. In addition, disorder is introduced by the partial occupation of the hydrogen sites. Spin-glass behaviour observed for $TbBrD_x$ with $x \simeq 0.7$ and a spin-glass freezing temperature of about 20 K gives strong evidence that the hydrogen vacancies are randomly distributed [10]. On the other hand, a very strong decrease of the conductivity of $GdBrD_x$ and $GdID_x$ for $x \rightarrow 0.7$ and below about 30 K apparently originating from a metal–insulator transition might be associated with hydrogen/vacancy ordering and the formation of a superstructure within the metal-atom planes [11]. Coherence of the superstructure along [001] is expected to be small since only weak van der Waals forces couple the X–RE–RE–X sheets.

These observations point to the fact that the behaviour of the hydrogen atoms plays an essential role for the physical properties of the hydride monohalides of the rare-earth elements. We have therefore investigated the hydrogen/deuterium vibrational spectra of $YBrH_x$, $TbBrH_x$, $TbClH_x$ and $YBrD_x$ ($x \simeq 0.8$ for all samples) by means of inelastic neutron spectroscopy.

In order to analyse the vibrational spectra quantitatively the exact metal-atom distances for the *particular host* are required. For $TbClD_x$ and $TbBrD_x$ ($x \simeq 0.8$) they are already available from the neutron structural work of Ueno *et al* and Cockcroft *et al* [13, 14]. For the non-magnetic compounds $YBrD_x$ a full structure determination has not been carried out so far. Therefore, in addition to the inelastic work a neutron diffraction experiment and structure refinement were carried out on a sample of $YBrD_{0.79}$.

## 2. Theory

A description of the vibrational properties of a hydrogen atom on an interstitial site in a metal-atom environment may start with the approximation of a spherically symmetric three-dimensional harmonic oscillator. Interactions with the atoms in the environment can be considered as a deviation from the spherical symmetry of the potential of a free three-dimensional harmonic oscillator and treated by perturbation theory [15].

To begin with, it is instructive to restrict the discussion to transitions from the ground state to the first excited state which for a three-dimensional spherically symmetric harmonic potential is threefold degenerate and can be characterized by the angular momentum $l = 1$. If the hydrogen atom occupies the centre of a regular tetrahedron as given e.g. for the rare-earth dihydrides with the $CaF_2$ structure the local symmetry is that of the cubic point group $T_d$. The hydrogen vibrations induce the irreducible representation $\Gamma_5$. The corresponding eigenstate is threefold degenerate, i.e. the degeneracy of the first excited level of a three-dimensional harmonic oscillator is not split by the action of a potential with

cubic symmetry. Consequently, a single optical hydrogen mode (transition from the ground to the first level) is observed for the rare-earth dihydrides.

In the hydride monohalides of the rare-earths the metal environment of a hydrogen atom is that of a tetrahedron which is slightly compressed along a threefold axis. The local symmetry of the hydrogen site is reduced to $3m$ (point group $C_{3v}$ (see table 1)). Reduction of the $\Gamma_5$ representation shows that it is the direct sum of the $\Gamma_1$ and $\Gamma_3$ irreproducible representations of $C_{3v}$. The threefold degeneracy thus is removed and two modes with intensity ratios 1 : 2 are expected with the $\Gamma_1$ mode shifted to higher energy.

The spectrum of the second-harmonic mode, in general, is slightly more intricate since the second excited level of a three-dimensional spherically symmetric harmonic oscillator contains s- and d-type wavefunctions and in total is sixfold degenerate. This degeneracy can already be removed by a potential of cubic symmetry. In a treatment analogous to the evaluation of the *crystal-field* splitting of the angular-momentum degeneracy of a free atom which is exposed to the crystal electric field of neighbouring atoms in a solid [16] Bennington *et al* have described how to obtain the splitting when the symmetry is reduced and degeneracies are lifted [17]. In a very convenient way this scheme allows one to parametrize the force fields (crystal electric fields) of the metal-atom environment.

One starts from the spherically symmetric three-dimensional harmonic oscillator. In polar coordinates its wavefunction $\psi_{nlm}$ can be written in terms of a radial part, $R_{nl}$, which essentially contains associated Laguerre polynomials $L^{l-1/2}_{(n-l-1)/2}(\beta r^2)$ where $\beta = (m\omega/\hbar)^2$ and $\hbar\omega$ is the energetic distance between the subsequent oscillator levels, and an angular-dependent part consisting of spherical harmonics $Y_{lm}(\Theta, \phi)$:

$$\Psi(r, \Theta, \phi) = R_{nl}(r)Y_{lm}(\Theta, \phi) \tag{1}$$

$$R_{nl} = N_{nl}r^l \exp(-\beta r^2/2)L^{l+1/2}_{(n-l-1)/2}(\beta r^2) \tag{2}$$

where $N_{nl}$ is a normalization factor.

The deviation from the spherically symmetric potential, $\Delta V$, due to the crystal field of the environment is expanded in a series of spherical harmonics (c.fe.g. [16])

$$\Delta V = \sum_{kq} a_{kq} r^k Y_{kq}(\theta, \phi) \tag{3}$$

where the coefficients of expansion $a_{kq}$ parametrize the *crystal field* (force field) of the environment. The number of $a_{kq}$ is limited by certain requirements of the surroundings: the expansion (3) may contain only spherical harmonics whose symmetry is compatible with the symmetry of the potential; the reality of $\Delta V$ requires $a_{kq} = (-1)^q a^*_{k-q}$; if there is a centre of inversion only even $k$ will be present.

In addition, due to properties of irreducible tensor operators, matrix elements vanish unless $k \leqslant 2l$. Thus, for the first excited level, only $a_{2q}$, and, for the second excited level, $a_{4q}$, need be considered.

The expansion (3) is treated in conventional degenerate perturbation theory. By diagonalizing the secular matrices for the individual excited level under consideration the energy eigenvalues are obtained in terms of of the crystal-field parameters $a_{kq}$. Conversely, by measuring the transition energies from the ground level to the split excited levels the crystal-field parameters can be obtained.

For a potential with $C_{3v}$ symmetry the first terms of the series (3) compatible with the symmetry of the potential are $Y_{20}$, $Y_{40}$ and $Y_{4\pm3}$. The set of expansion coefficients, $a_{20}$, $a_{40}$ and $a_{4\pm3}$ is sufficient to describe the energies of the states up to the second excited level containing $l$ = 0- and $l$ = 2-type wavefunctions. For the first excited level with $l$ = 1 only $Y_{20}$ has non-zero matrix elements and the coefficient and $a_{20}$ can be gained.

The excitation energies, $E_{01}$ and $E_{02}$, from the ground level to the first excited level as calculated from the secular matrices by Bennington *et al* are the doubly degenerate mode at energy [17]:

$$E_{01} = \hbar\omega - \tfrac{1}{2}\sqrt{5}\alpha \tag{4}$$

and the single mode at

$$E_{02} = \hbar\omega + \sqrt{5}\alpha \tag{5}$$

using the abbreviation

$$\alpha = \frac{a_{20}}{\beta}\sqrt{1/4\pi}. \tag{6}$$

The splitting

$$E_{02} - E_{01} = \frac{3}{2\beta}\sqrt{\frac{5}{4\pi}}a_{20} \tag{7}$$

is determined by the quadrupolar parameter $a_{20}$ and the energy gap between unperturbed oscillator levels is given by

$$\hbar\omega = \tfrac{1}{3}(2E_{01} - E_{02}). \tag{8}$$

Excitation energies to states of the second excited level which remains partially degenerate are

$$E_{1\pm1} = 2\hbar\omega + \tfrac{1}{2}\sqrt{5}\alpha + \tfrac{27}{4}\gamma \pm \tfrac{1}{2}\sqrt{W_1} \tag{9}$$

$$E_{3\pm1} = E_{2\pm1} = 2\hbar\omega + \tfrac{1}{4}\sqrt{5}\alpha + \tfrac{27}{8}\gamma \pm \tfrac{1}{2}\sqrt{W_2} \tag{10}$$

where

$$W_1 = (\sqrt{5}\alpha + \tfrac{27}{2}\gamma)^2 - 49\gamma^2 \tag{11}$$

$$W_2 = (\tfrac{3}{2}\sqrt{5}\alpha + \tfrac{45}{4}\gamma)^2 + \tfrac{2835}{4}\delta^2 \tag{12}$$

$$\gamma = \frac{a_{40}}{\beta^2}\sqrt{1/4\pi} \tag{13}$$

and

$$\delta = \frac{a_{43}}{\beta^2}\sqrt{1/4\pi}. \tag{14}$$

In a potential of $C_{3v}$ symmetry the second excited level is split into four states. Their energies are determined by the parameters $\alpha$, $\gamma$ and $\delta$ which can be obtained from a least-squares fit of the observed transition energies.

For the case of a small orthorhombic distortion to the $C_{3v}$ symmetry, additional terms, $Y_{2\pm2}$ and $Y_{4\pm2}$, enter the expansion (3) and lead to a further loss of degeneracy.

## 3. Experimental details

Powder samples were prepared according to standard procedures described in detail previously [19]. Hydrogen and deuterium contents were analysed chemically with an accuracy of 3% [18]. For the case of the deuterated compound, $YBrD_x$, $x$ was simultaneously obtained from the diffraction experiment (see details below). The two concentrations within experimental error were identical.

For the neutron diffraction measurements, approximately 2 g of $YBrD_{0.79(2)}$ (D concentration according to chemical analysis) was filled in a 9 mm thin-walled vanadium

sample can. Diffraction patterns were collected at the Institut Laue–Langevin, Grenoble, on the high-resolution diffractometer D2B (wavelength 1.595 Å) at 1.5 K in the $2\theta$-range 6–156° (in steps of 0.05°) in about 20 h.

Inelastic neutron spectra were acquired on the high-resolution inelastic spectrometer IN1BeF at the ILL equipped with a liquid-nitrogen cooled Be filter in the energy range 40–210 meV using Cu(220) monochromatization. To correct for the finite cut-off of the Be filter an approximate value of 4 meV was subtracted from the incident energy.

For the inelastic scattering experiments $\simeq$ 1 g of $YBrH_{0.75}$, $TbBrH_{0.83}$ and $TbClH_{0.83}$ and $\simeq$ 2 g of $YBrD_{0.79}$ (two samples) were sealed in thin-walled quartz glass containers which were designed to provide flat samples with a thickness of $\simeq$ 1 mm for the hydrogenated and $\simeq$ 2 mm for the deuterated compounds, respectively. An empty quartz sample container was measured in a separate run and the value subtracted.

## 4. Results and discussion

### *4.1. Diffraction*

The structure of $YBrD_{0.79}$ was refined by the Rietveld method [20] in the rhombohedral space group $R\bar{3}m$ (No 166, hexagonal setting) using the program PROFIL [21] from the D2B data collected at 1.5 K (figure 1).

From the 3050 data points containing 126 contributing reflections, a total of 15 parameters (of which seven are structural) were refined. The final parameters are listed in table 1.

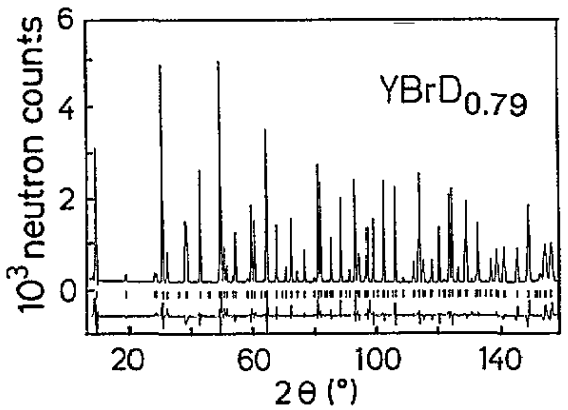


**Figure 2.** Observed, calculated and difference profiles for $YBrD_{0.79}$ at 10 K measured on D1A with $\lambda$ = 1.911 Å. Vertical tick marks indicate calculated reflection positions. The background was estimated by graphical methods.

**Table 1.** Final parameters, *R*-factors, and interatomic distances for $YBrD_{0.79}$ at 10 K. *R*-factors are defined as by Rietveld [20] with $y_i$(obs) referring only to the Bragg intensity, i.e. $y_i$(obs) = $y_i$(total) − $y_i$(background). Weights are given by $1/\sigma^2_{y(\mathrm{obs})}$. Scattering lengths Y = 7.75 fm, D = 6.674 fm, Br = 6.80 fm were taken from [22]. $\lambda$ = 1.595 Å. Space group $R\bar{3}m$ (hexagonal setting). Lattice parameters $a$ = 380.469(2) pm, $c$ = 2881.93(6) pm. $U$, $V$, $W$ ($^{\circ 2}$): 0.068(2); −0.168(6); 0.198(3); $R_{wp}$ = 14.9%; $R_{exp}$ = 1.9%; $R_I$ = 6.51%.

| Atom | Site symmetry | | $x$ | $y$ | $z$ | $B$ (Å$^2$) | $N$ |
|---|---|---|---|---|---|---|---|
| Y | 2d | $3m$ | 0 | 0 | 0.11950(1) | 0.29(3) | 1 |
| Br | 2d | $3m$ | 0 | 0 | 0.38815(1) | 0.33(3) | 1 |
| D | 2d | $3m$ | 0 | 0 | 0.1963(1) | 0.82(6) | 0.773(8) |

The layered structure (isotypic to the ZrCl structure type [23]) is based on a metal bilayer interspaced with bromine bilayers. The deuterium interstitials occupy the tetrahedrally coordinated sites in the metal-atom bilayer. The deuterium occupation factor refined to 0.77(1) which within experimental error is identical to the value obtained from chemical analysis. Within experimental limits no evidence for occupation of the octahedral sites was found.

An extensive discussion of the crystal structures of the hydride monohalides of the rare earths can be found in the chapter by Simon *et al* [9]. Here, we summarize relevant features for a quantitative comparison of the spectra:

(i) The first coordination shell of a deuterium atom consists of a slightly distorted metal atom-tetrahedron. The metal-atom environment of a deuterium atom in $YBrD_{0.79}$ is sketched in figure 3.

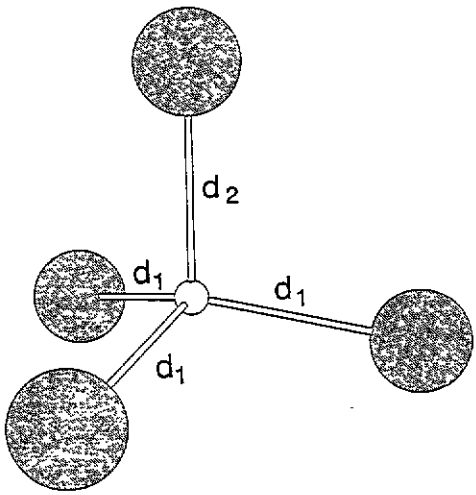


**Figure 3.** First-coordination-shell metal-atom environment of a hydrogen (deuterium) atom in the rare-earth monohalide hydrides. $d_i$ refer to the distances as given in table 2.

(ii) The distance ($d_2$, for labelling cf. figure 3) of the deuterium atom to the apex metal atom is about 2% smaller than the distance to the metal atoms in the triangular basis. The distances from a deuterium atom to the metal atoms in the triangular basis ($d_1$) are almost identical to the deuterium–metal distance observed in fluorite-type $YD_2$ [24]. Table 2 summarizes the metal-to-hydrogen (deuterium) distances in the REXH(D)$_x$ compounds investigated in this work. For the case of the compound $TbClH_{0.83}$ the difference in the distances from the hydrogen atoms to the four metal atoms is smallest i.e. the deviation from the perfect tetrahedral environment almost vanishes for $TbClH_{0.83}$.

**Table 2.** Hydrogen–metal-atom distances in $YBrD_{0.79}$, $TbBrD_{0.81}$ and $TbClD_{0.8}$ according to the results of neutron-diffraction investigations. The distances $d_i$ are defined as in figure 3.

| Compound | Reference | $T$ (K) | $z_M$ | $z_D$ | $a$ (pm) | $c$ (pm) | $d_1$ (pm) | $d_2$ (pm) |
|---|---|---|---|---|---|---|---|---|
| $YBrD_{0.79}$ | this work | 1.5 | 0.11950(5) | 0.1963(1) | 380.469(2) | 2881.93(6) | 225.4(1) | 221.3(3) |
| $TbBrD_{0.81}$ | [14] | 2 | 0.11902(7) | 0.19648(9) | 383.022(1) | 2890.8(2) | 227.1(1) | 223.9(3) |
| $TbClD_{0.8}$ | [13] | 293 | 0.2169(1) | 0.1358(1) | 378.00(5) | 2749.4(4) | 224.7(4) | 223.0(8) |

### *4.2. Inelastic scattering*

The spectra of $YBrH_{0.75}$ and $TbBrH_{0.83}$ consist of a doublet with the low-energy mode approximately twice as intense as the high-energy mode. The centre of gravity is located at energies around 125 meV and matches very well the values observed for the rare-earth metal dihydrides [6].

The linewidth (FWHM) is about 8 meV, with the low-energy mode being approximately 30% broader than the high-energy mode. The spectrum of $TbClH_{0.83}$ exhibits a single asymmetric line only. It has a width of approximately 12 meV and is centred at about 128 meV. The linewidth and the shoulder on the high-energy side indicate that the mode is also composed of two overlapping lines. Figure 4 compares the spectra of $YBrH_{0.75}$, $TbBrH_{0.83}$ and $TbClH_{0.83}$ all obtained at 10 K.

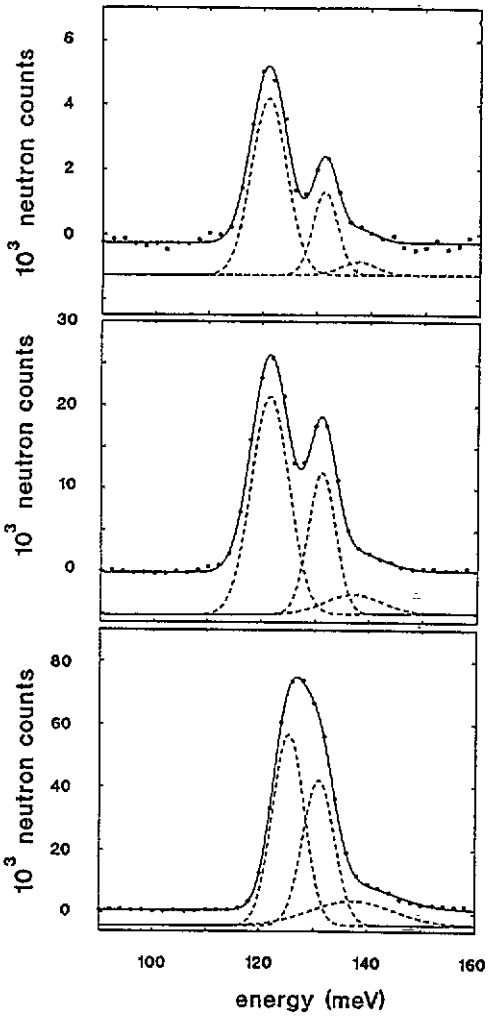


**Figure 4.** IN1BeF neutron spectra of $YBrH_{0.75}$, $TbBrH_{0.83}$ and $TbClH_{0.83}$ (from top to bottom) at 10 K. Solid lines represent the result of the fits using three Gaussian lines which are indicated by the broken lines (origin shifted).

The hydrogen modes are surprisingly well resolved in view of the fact that concentrated hydride compounds are present. The width of the modes is essentially resolution limited [25]. The broadening of the low-energy mode with respect to the high-energy mode will be discussed below. The characteristic splitting of the peaks in the spectra of the investigated hydride compounds and the centre of gravity of the mode energies proves that the hydrogen

atoms occupy the tetrahedrally coordinated lattice sites in the metal-atom bilayer as was concluded from the diffraction experiments. No indication of weak modes around 60 meV was found in the spectra of $YBrH_{0.75}$ and $TbBrH_{0.83}$. For $TbClH_{0.83}$ alone a very weak feature centred at about 65 meV and of less than 1% of the total intensity might indicate a very slight occupation of the octahedral sites. However, significant occupation of the octahedral sites in the rare-earth metal dihydrides is only detected if all of the available tetrahedral sites are almost completely filled. This is not the case in the present system. We prefer to attribute this feature to an imperfect subtraction of the background resulting from the quartz sample holder. As was shown in a recent detailed neutron study of the vibrational density of states of quartz glass [26], and as can be seen from the reference measurement of our quartz sample holders, there is structure and a peak in the relevant energy range of the spectrum of quartz which could account for the observed feature.

The spectra were evaluated quantitatively by fits with a Gaussian peak-shape function. Satisfying fits could be obtained using two overlapping Gaussian functions with the individual intensities, linewidth and centre as free parameters. For the spectrum of $TbClH_{0.83}$ identical linewidths had to be assumed for both modes. The spectrum of $TbClH_{0.83}$ clearly exhibits an additional tail on the high-enery side of the mode which is attributed to acoustic sidebands as frequently observed in hydride optical spectra [27]. A closer inspection of the difference of the two-line fits to the experimental spectra reveals tails also in the spectra of $YBrH_{0.75}$ and $TbBrH_{0.83}$. In the fits the sidebands can be successfully accounted for by adding a third Gaussian centred at about 137 meV with an intensity of about 10% of the total intensity. Adding a third Gaussian significantly improves the $R$-factors of the fits but only changes slightly the parameters of the strong modes as gained from the two-line fit (table 3).

**Table 3.** Excitation energies $E_{0i}$, linewidth $\Delta E_i$ (FWHM) and intensities $I_i$ of the hydrogen optical modes in $YBrH_{0.75}$, $TbBrH_{0.83}$ and $TbClH_{0.83}$. The spectrum of $TbClH_{0.83}$ was fitted under the constraint of equal linewidths.

| Compound | $T$ (K) | $I_1$ ($10^3$ a.u.) | $E_{01}$ (meV) | FWHM$_1$ (meV) | $I_2$ ($10^3$ a.u.) | $E_{02}$ (meV) | FWHM$_2$ (meV) | $I_3$ ($10^3$ a.u.) | $E_{03}$ (meV) | FWHM$_3$ (meV) |
|---|---|---|---|---|---|---|---|---|---|---|
| $YBrH_{0.75}$ | 10 | 5.52 | 121.0(1) | 7.8(2) | 2.59 | 131.4(1) | 5.3(2) | 0.48 | 137.4(2) | 7.4(3) |
| $TbBrH_{0.83}$ | 10 | 26.1 | 121.5(1) | 8.2(2) | 16.9 | 131.2(1) | 6.0(2) | 2.32 | 137.0(2) | 12.4(5) |
| $TbClH_{0.83}$ | 10 | 60.8 | 125.4(1) | 6.9(2) | 46.2 | 131.0(1) | 6.9(2) | 7.9 | 137.2(3) | 18.1 (5) |

As becomes evident already from figure 4 the splitting of the modes reduces increasingly in the series $YBrH_{0.75} \rightarrow TbBrH_{0.83} \rightarrow TbClH_{0.83}$. This tendency reflects the decreasing distortion of the metal atom tetrahedra of the first coordination shell in the respective compounds (table 2).

The magnitude of the splitting ($E_{20}$-$E_{10}$, $\alpha$ and equivalently the quadrupolar expansion parameter $a_{20}$ (cf. (6)) is smaller than in $YH_{0.11}$ [17] and of opposite sign. To a good approximation it depends linearly on the difference ($d_1$-$d_2$; cf. table 2) of the two hydrogen-to-metal distances (figure 5) which can be considered as a measure of the deviation from an ideal tetrahedral coordination. Thus

$$E_{02} - E_{01} = 2.8(1)\ \text{pm eV}^1(d_1 - d_2)$$

which implies a power law dependence

$$E(\text{meV}) = Ad\ (\text{pm})^{2.8(1)}$$

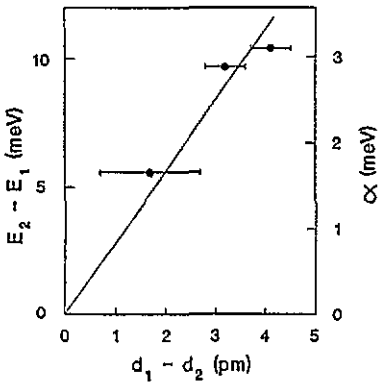


**Figure 5.** Splitting of the hydrogen modes ($E_{02}$-$E_{01}$) of the investigated rare-earth monohalide hydrides versus the difference between the hydrogen distances from the apex metal atom ($d_2$) and the metal atoms in the triangular basis ($d_1$).

with $A = 4.9(1) \times 10^8$ meV, significantly different from the power law suggested by Ross *et al* when correlating the fluorite-structure-type dihydrides of transition and rare-earth metals [7].

However, given the limited subset of the rare-earth dihydrides, we find good agreement for the power law, $\propto d^{2.8}$, with deviations of less than 3%.

The results of the fits verify that the reduced broadening is mainly due to a growth of the resonance energy of the low-energy mode whereas the high-energy mode undergoes a slight move towards lower energies only. These trends are paralleled by the sequence of metal-to-hydrogen distances in the terbium compounds, $TbBrH_{0.83}$ and $TbClH_{0.83}$ (cf. table 2). The metal-to-hydrogen distances for $YBrH_{0.75}$ do not follow this trend, this might be related to the difference in the electronic configuration of Y and Tb.

The results of the detailed quantitative evaluation of the spectra (cf. table 3) also reveal that the intensity of the high energy modes is somewhat reduced compared to the ideal ratio 2:1. This finding points to a pronounced anisotropy of the Debye–Waller factor due to enhanced contributions to the Debye–Waller factor from band modes vibrating in the *c*-direction as may be expected for a layer–type crystal structure.

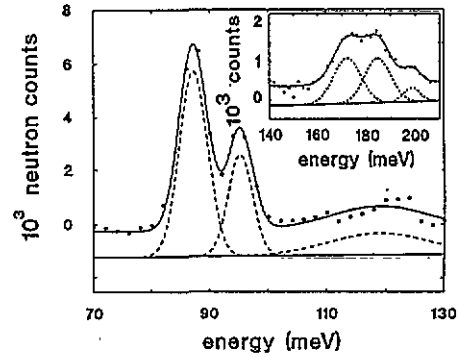


**Figure 6.** IN1BeF neutron spectrum of $YBrD_{0.79}$ at 10 K. The inset displays the second harmonic transitions on an enlarged scale. The solid line represents the result of the fit using Gaussians which are given by the broken lines (origin shifted).

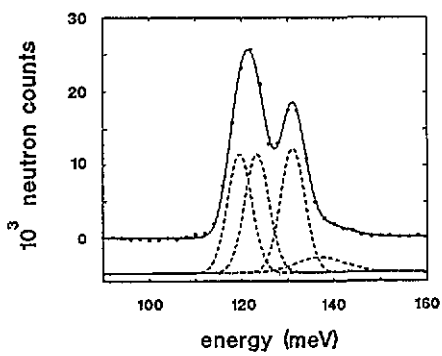


**Figure 7.** IN1BeF neutron spectra of $TbBrH_{0.83}$ Solid lines represent the result of the fits using four Gaussian lines which are indicated by the broken lines. The three strong lines were assumed to have identical linewidth, the two low-energy lines were assumed to have identical intensity.

The essential features in the spectrum of $YBrD_{0.79}$ (figure 6) besides a downshift of the energy scale by about a factor of $\sqrt{2}$ are identical to those of the hydride spectra. The low-energy mode is still broader than the high-energy mode, but the difference in width between

**Table 6.** Excitation energies $E_{0i}$, linewidth $\Delta E_i$ (FWHM) and intensities $I_i$ of the second harmonic transitions in $YBrD_x$.

| Compound | $T$ (K) | $I_3$ ($10^3$ a.u.) | $E_{03}$ (meV) | FWHM$_3$ (meV) | $I_4$ ($10^3$ a.u.) | $E_{04}$ (meV) | FWHM$_4$ (meV) | $I_5$ ($10^3$ a.u.) | $E_{05}$ (meV) | FWHM$_5$ (meV) |
|---|---|---|---|---|---|---|---|---|---|---|
| $YBrD_{0.79}$ | 10 | 1.18 | 172.0(4) | 13.3(6) | 1.15 | 184.7(6) | 12.7(7) | 0.37 | 198.6(10) | 8.0(7) |
| $YBrD_{0.81}$ | 10 | 0.91 | 171.2(6) | 10.8(5) | 1.01 | 183.8(6) | 13.9(7) | 0.26 | 200.3(11) | 11.6(8) |

the low- and high-energy modes is significantly less pronounced than in the hydride spectra. The linewidth of the low-energy mode growsslightly upon raising the sample temperature to 100 K while the linewidth of the high energy mode does not change.

**Table 4.** $\hbar\omega$ and $\alpha$ for the hydrogen optical modes in $YBrH_{0.75}$, $TbBrH_{0.83}$ and $TbClH_{0.83}$. and $\alpha$ For comparison values for $YH_{0.11}$ as obtained in [17] are also listed.

| Compound | Reference | $\hbar\omega$ (meV) | $\alpha$ (meV) |
|---|---|---|---|
| $YBrH_{0.75}$ | this work | 124.5 | 3.1 |
| $TbBrH_{0.83}$ | this work | 124.7 | 2.9 |
| $TbClH_{0.83}$ | this work | 127.3 | 1.7 |
| $YH_{0.11}$ | [17] | 122.2 | −11.0 |

In contrast to all hydride spectra, there is no weak (*third*) line on the high-energy side of the second mode. Besides the two strong modes between 87 meV and 95 meV a very weak feature centred at around 125 meV is detected for the deuterium compounds. We ascribe it to a trace (approximately 1%) contamination due to hydrogen atoms. In addition, three weak modes were found between 160 meV and 200 meV (see inset figure 6) which we attribute to transitions to states of the second harmonic level. Their integrated intensity amounts to about 20% of the first harmonic transition.

**Table 5.** Excitation energies $E_{0i}$, linewidth $\Delta E_i$ (FWHM) and intensities $I_i$ of the deuterium optical modes in two samples of $YBrD_x$.

| Compound | $T$ (K) | $I_1$ ($10^3$ a.u.) | $E_{01}$ (meV) | FWHM$_1$ (meV) | $I_2$ ($10^3$ a.u.) | $E_{02}$ (meV) | FWHM$_2$ (meV) |
|---|---|---|---|---|---|---|---|
| $YBrD_{0.79}$ | 10 | 6.95 | 87.1(1) | 5.7(2) | 3.80 | 95.2(1) | 5.0(2) |
| $YBrD_{0.81}$ | 10 | 4.09 | 87.0(1) | 5.6(2) | 2.39 | 94.9(1) | 5.2(2) |
| $YBrD_{0.81}$ | 100 | 3.69 | 86.9(1) | 6.1(2) | 2.40 | 94.9(1) | 5.2(2) |

The results of the least-squares fits (cf. table 5) indicate a splitting parameter $\alpha$ of the first harmonic level of

$$\alpha = 2.4(1)\ \text{meV}$$

and an energy distance of the unsplit levels of

$$\hbar\omega = 89.8\ \text{meV}.$$

The ratio

$$\hbar\omega_H/\hbar\omega_D = 1.388(5)$$

is slightly lower than the harmonic ratio of $\sqrt{m_D/m_H} = \sqrt{2}$ indicating a small anharmonicity of the potential. Ratios very close to $\sqrt{2}$ are also found for the related modes in the hydride and deuteride spectra indicating that the force constants do not differ appreciably for the two isotopes.

From a least-squares fit of the second-harmonic mode energies assuming that the energy of the more intensive modes ($E_{03}$ and $E_{04}$, cf. table 6) is given by (10) and the highest energy mode $E_{05}$ corresponds to (9) $\gamma$ and $\delta$ were determined as

$$\gamma = 1.0(2) \text{ meV} \qquad |\delta| = 1.2(2) \cdot 10^{-3} \text{ meV}.$$

In order to successfully fit the second-harmonic modes, a reduction of $2\hbar\omega$ by 3% has to be taken into account, indicating again an anharmonicity of the potential. With these parameters the experimental and fitted mode energies are (with fitted values in parenthesis): 87.1 (87.1) meV, 95.2 (95.2) meV, 172.0 (171.9) meV, 184.7 (191.4) meV, 198.6 (195.3) meV.

We now turn to a discussion of the significant linewidth difference between the low- and high-energy modes of the first harmonic transition. It is similarly present in both hydride and deuteride spectra, but is noticeably more pronounced in the hydrogen systems. Since the broadening cannot be explained as due to different instrumental resolution in the relevant energy ranges [25], it must be of microscopic origin. A straightforward explanation is based on a slight splitting of the doubly degenerate low-energy mode. The splitting is too small to be resolved but leads to broadening of the mode. The evident origin of the splitting is a reduction of the local symmetry from $C_{3v}$ brought about by local inhomogeneities (lattice distortions) which are induced by vacancies in the hydrogen/deuterium sublattice. This presumption gains some support from the temperature dependence of the linewidth of $YBrD_{0.79}$ spectrum when raising the temperature from 10 K to 100 K. While the linewidth of the high-energy mode (vibration along the threefold axis) stays the same, the linewidth of the low-energy mode increases by 9%. This small, but perceptible, increase indicates a phononic origin of the broadening of the in-plane mode implying some sensitivity to lattice distortions around the vibrating hydrogen/deuterium atom. If the splitting were caused by hydrogen/deuterium–hydrogen/deuterium interactions the temperature dependence might be expected to be less pronounced.

The reduction from local $C_{3v}$ symmetry e.g. by an orthorhombic distortion can be accounted for by the addition of a $a_{22}Y_{22}$ term to expansion (3) which leads to the removal of all degeneracies and consequently the splitting of the doubly degenerate low-energy mode (cf. [17]).

The result of hydride/deuteride vacancies on the lattice relaxation is smaller for the less voluminous deuterium atom. In consequence, the distortion of the metal tetrahedra is smaller for the deuteride compounds leading to a reduced splitting of the low-energy mode as found for $YBrD_x$ compared to $YBrH_x$.

For hydrogen/deuterium concentrations with $x \simeq 0.8$ as for all the investigated samples, and assuming a random distribution of the vacancies and neglecting any interaction between the vacancies, the probability of finding one, two or three vacant sites in the first hydrogen/deuterium coordination shell is about 38%, 10% and 1%, respectively. The completely filled environment is still the most likely one (51%). Thus, assuming that the splitting is determined essentially by the distortion induced by the vacancies in the first hydrogen/deuterium coordination shell, the resulting spectrum can be simulated as a superposition of one resolution-limited single mode and three twofold modes. Their integrated intensity is given according to the above probabilities. A simulation of the spectra with these assumptions resulted in significantly improved fits even if only the two most likely contributions (undistorted neighbourhood and a single vacancy) were taken into account.

However, a more simple approach, namely assuming a simple splitting of the low-energy mode into two lines of approximately the same intensity and the constraint of identical linewidth for all three strong modes leads to equally good fits (figure 7). Both ways to

simulate the broadening point to a splitting of the low-energy mode of 3.7(2) meV for $TbBrH_{0.83}$ and 3.8(2) meV for $YBrH_{0.75}$. As expected from the smaller linewidth difference in the deuterium spectra, a deconvolution of the spectrum of $YBrD_{0.79}$ indicates a splitting of 1.53(2) meV. Using as a first approximation the linear splitting–distance relationship found for the fundamental splitting of the hydrogen spectra of the rare-earth monohalide hydrides, these values imply distortions of the metal-atom tetrahedra of about 1.2 pm which, however, are considerably smaller than observed e.g. in rare-earth hydrides [28].

This discrepancy indicates that the broadening of the doubly degenerate mode could rather originate from hydrogen-hydrogen interaction leading to some dispersion of the optical branch. Hydrogen-hydrogen interaction, on the other hand, may lead to an ordering of the vacancies within a metal-atom double layer forming a superstructure in the $a$–$b$ plane with reduction of the local symmetry and a splitting of the degenerate level. There is no support from diffraction experiments, so far, for this presumption [14]. However, a detection of such an ordering e.g. by diffraction techniques might be prevented due to loss of coherency along [001] as a consequence of the weak interlayer coupling. On the other hand, an NMR investigation on the structurally equivalent compounds $ZrXH_{0.5}$ (X = Cl, Br) pointed to an ordering of the hydrogen atoms into alternate chains [29].

In conclusion, from the present data and analysis one cannot conclusively decide which of the two models reflects the true situation. A lowering of the local symmetry from $C_{3v}$ due to distortions induced by hydrogen vacancies or even by vacancy ordering may be present. Vacancy ordering seems possible and would be a very interesting phenomenon to study e.g. by temperature-dependent measurements to find the transition to a disordered phase. The analysis of the broadening of the mode allows some conclusions about the size of the displacement of the metal atoms induced by the vacancies. Distortions vanish for samples with $x \simeq 1$ and the low-energy mode can be expected to narrow. Dispersion of the low-energy mode due to hydrogen-hydrogen interactions can be expected to be present also for $x \to 1$. Experiments on samples with $x \simeq 1$ which should give more insight into the problem are scheduled.

## 5. Summary

In summary, our first investigation of the local modes of hydrogen and deuterium atoms in a series of hydride (deuteride) monohalides of the rare-earth elements, $REXH_x$, with RE = Y and Tb, X = Cl and Br and $x \simeq 0.8$ by means of inelastic neutron scattering represents an instructive example of the hydrogen/deuterium vibrational properties in new and unusual two-dimensional metallic hosts. An increasing splitting of the triply degenerate first-harmonic transition into two modes due to a growing compression of the tetrahedrally coordinated hydrogen/deuterium lattice site along a threefold axis is correlated with hydrogen/deuterium to metal-atom distances in the particular host.

The analysis of the spectra including second-harmonic transitions observed for the case of the deuteride spectra in terms of crystal-field theory allows a convenient parametrization of the force constants and an instructive comparison with structurally related rare-earth dihydrides.

Characteristic broadenings of the linewidth of the low-energy modes are observed. Possible sources of these broadenings are named and discussed.

## Acknowledgments

We thank R Eger and B Bending for help with the sample preparation. Helpful discussions

with S M Bennington, Chr Elsässer, T H Metzger, U Stuhr and H Wipf are gratefully acknowledged.

## References

[1] See e.g. Fukai Y 1993 *The Metal Hydrogen System* (Berlin: Springer) ch 4
[2] See e.g. Alefeld and Völkl J 1978 *Hydrogen in Metals I* (Berlin: Springer) ch 4
[4] See the compilation of data Kress W 1987 *Fachinformationszentrum Karlsruhe* No 26-1
[5] *Landolt–Börnstein New Series* 1991 Group III vol 19 (Berlin: Springer) p 280
[6] Sakamoto M 1961 *J. Phys. Soc. Japan* **19** 1862
[7] Hunt D G and Ross D K 1976 *J. Less-Common Met.* **49** 176
[8] Ross D K, Martin P F, Oates W A and Khoda Bakhsh R 1979 *Z. Phys, Chem.* **114** 221
Anderson I S, Rush J J, Udovic T J and Rowe J M 1986 *Phys. Rev. Lett.* **57** 2822
Anderson I S, Berk N F, Rush J J and Udovic T J 1988 *Phys. Rev.* B **37** 4358
Udovic T J, Rush J J, Anderson I S and Barnes R G 1990 *Phys. Rev.* B **41** 3460
[9] Simon A, Mattausch Hj, Miller G J, Bauhofer W and Kremer R K *Handbook on the Physics and Chemistry of Rare Earths* vol. 15, ed K A Gschneidner Jr and L Eyring (Amsterdam: North-Holland)
[10] Kremer R K, Bauhofer W, Mattausch Hj, Brill W and Simon A 1990 *Solid State Commun.* **73** 281
Kremer R K, Bauhofer W, Mattausch Hj and Simon A 1991 *Eur. J. Inorg. Solid State Chem.* T **28** 519
[11] Bauhofer W, Joss W, Kremer R K, Mattausch Hj and Simon A 1992 *J. Magn. Magn. Mater.* **104-107** 1243
[12] Stuhr U, Wipf H, Kremer R K, Mattausch Hj and Simon A *J. Phys.: Condens. Matter* at press
[13] Ueno F, Ziebeck K, Mattausch Hj and Simon A 1984 *Rev. Chim. Miner.* **21** 804
[14] Cockcroft J K, Bauhofer W, Mattausch Hj and Simon A 1989 *J. Less-Common Met.* **152** 227
[15] For limitations of the applicability of perturbation theory for the case of hydrogen vibrational properties in metals (here Pd) cf. e.g. Elsässer C, Ho K M, Chan C T and Fähnle M 1991 *Phys. Rev.* B **44** 10377
[16] Abragam A and Bleaney B 1970 *Electron Paramagnetic Resonance of Transition Metal Ions* (Oxford: Oxford University Press) ch 16
[17] Bennington S M, Ross D K, Benham M J, Taylor A D, Bowden Z A and Osborn R 1990 *Phys, Lett.* **151A** 325
Bennington S M and Ross D K *preprint*
[18] Eger R, Mattausch Hj and Simon A 1993 *Z. Naturf.* b **48** 48
[19] Mattausch Hj, Schramm W, Eger R and Simon A 1985 *Z. Anorg. (Allg.) Chem.* **530** 43
[20] Rietveld H M 1969 *J. Appl. Cryst.* **2** 65
[21] Cockcroft J K 1991 PROFIL *V4.05: A Rietveld Program for the Refinement of Crystal Structures from Single and Multiphase Powder Neutron and Synchrotron Radiation Data* (Grenoble: Institut Laue Langevin)
[22] Koester L and Rauch H 1983 *IAEA Report* No. 2517/RB (Vienna: International Atomic Energy Agency)
[23] Adolphson D G and Corbett J D 1976 *Inorg. Chem.* **15** 1820
[24] Khatamian D, Kamitakahara W A, Barnes R G and Peterson D T 1980 *Phys. Rev.* B **21** 2622
[25] Almairac R, Prefaut J L, Galtier M, Benoit C, Montanier A and Lauter H J 1981 *Mol. Cryst. Liq. Cryst.* **69** 171
Lauter H J and Jobic H 1984 *Chem. Phys. Lett.* **108** 393
[26] Arai M, Hannon A C, Taylor A D, Wright A C, Sinclair R N and Price D L 1992 *Physica* B **180 & 181** 779
[27] Hempelmann R and Richter D 1981 *Z. Phys.* B **44** 159
[28] Metzger T H, Vajda P and Daou J N 1985 *Z. Phys. Chem.* **143** 129
[29] Hwang T Y, Schoenberger R J, Torgeson D R and Barnes R G 1983 *Phys. Rev.* B **27** 27. The possibility of deuterium/vacancy ordering in $TbBrD_x$ is discussed in [14].